

# Multimodal Language and Graph Learning of Adsorption Configuration in Catalysis

Janghoon Ock,<sup>†</sup> Srivathsan Badrinarayanan,<sup>†</sup> Rishikesh Magar,<sup>‡</sup> Akshay Antony,<sup>‡</sup> and Amir Barati Farimani<sup>\*,‡</sup>

<sup>†</sup>*Department of Chemical Engineering, Carnegie Mellon University, 5000 Forbes Street, Pittsburgh, PA 15213, USA*

<sup>‡</sup>*Department of Mechanical Engineering, Carnegie Mellon University, 5000 Forbes Street, Pittsburgh, PA 15213, USA*

E-mail: barati@cmu.edu

## Abstract

Adsorption energy is a reactivity descriptor that must be accurately predicted for effective machine learning (ML) application in catalyst screening. This process involves determining the lowest energy across various adsorption configurations on a catalytic surface, which can exhibit very similar energy values. While graph neural networks (GNNs) have shown great success in computing the energy of catalyst systems, they rely heavily on atomic spatial coordinates. In contrast, transformer-based language models can directly use human-readable text inputs, potentially bypassing the need for detailed atomic positions. However, these language models often struggle with accurately predicting the energy of adsorption configurations. Our study addresses this limitation by introducing a self-supervised multi-modal learning approach called graph-assisted pretraining, which connects well-established GNNs with emerging language model applications. This method reduces the MAE of energy prediction

for adsorption configurations by about 10%. Furthermore, our findings demonstrate that graph-assisted pretraining enhances fine-tuning with different datasets, indicating the transferability of this approach. This method also redirects the model’s attention toward adsorption configuration, rather than individual adsorbate and catalyst information, similar to common domain knowledge. Building on this, we propose using generative large language models to create text inputs for the predictive model, based solely on chemical composition and surface orientation, without relying on exact atomic positions. This demonstrates a potential use case of language models in energy prediction without geometric information.

**Keywords:** Computational Catalysis, Catalyst Screening, Multi-modal Model, Machine Learning, Transformer, Large Language Model

## Introduction

Machine learning (ML) approaches, particularly Graph Neural Networks (GNNs), have emerged as efficient surrogates to computationally expensive Density Functional Theory (DFT) simulations.<sup>1-4</sup> These advancements can accelerate energy and force predictions for high-throughput material screening.<sup>5-8</sup> The successful application of ML-based DFT surrogate modeling in catalysis can enable the identification of optimal catalyst materials for specific reactions, which is crucial for advancing energy storage technologies and sustainable chemical processes. The importance of such techniques has drawn attention beyond the chemical engineering and chemistry communities, extending into the AI for Science field.<sup>9</sup>

Despite the significant success of GNNs in machine learning applications in the catalysis domain, obtaining their input data can be challenging since they require precise atomic positions. Constructing graph representations of structures relies on identifying nearest neighbors within specific proximity thresholds for each atom.<sup>10-13</sup> However, achieving such precise coordinates can be difficult, limiting the applicability of GNNs primarily to theoretical studies. For instance, even with experimentally validated adsorption energy data from the

literature, using this information in modeling remains difficult because replicating the exact atomic positions of the adsorbate-catalyst systems from experiments is problematic.<sup>14,15</sup>

Recent advancements in language model applications offer a promising alternative to relying on exact atomic coordinates as input data.<sup>16–19</sup> Language models can process human-readable text descriptions of atomic systems instead of building an input with atomic coordinates. For example, the MOFormer model encodes metal-organic frameworks (MOFs) as text string representations, called MOFid, which include chemical information on building blocks and topology codes, unlike graph representations.<sup>16</sup> The TransPolymer model encodes polymers using the SMILES strings of their repeating units along with attributes such as the degree of polymerization, polydispersity, and chain conformation.<sup>18</sup> Additionally, the ability to process textual input allows us to incorporate experimentally-obtainable attributes into the input data. We aim to extend these successes from the materials science domain to the catalysis domain. For instance, the CatBERTa model takes textual input for adsorbate-catalyst systems to predict the energy of the system.<sup>19</sup>

Identification of adsorption energy is an important task in catalysis since it is a key reactivity descriptor in catalyst screening.<sup>3,20,21</sup> A single adsorbate-catalyst pair can have numerous adsorption configurations, varying by adsorption site and molecule orientation on the catalytic surface.<sup>8,22</sup> The minimum energy among these configurations is considered the adsorption energy. Due to the subtle differences between these configurations, their energies can be very similar. Therefore, to accurately identify the adsorption energy, the model must be capable of distinguishing these subtle energy differences, which can range from 0.1 to 0.3 eV around the minimum energy.<sup>8</sup> Even though the language model opens up the possibility of bypassing the need for exact atomic positions, its accuracy should be enhanced to apply this language-based approach to adsorption configuration energy prediction tasks.

To address this challenge, our study introduces graph-assisted pretraining, a multimodal learning method that leverages graph modality to improve the prediction accuracy of the language model for adsorption configurations. Multimodal learning has already been suc-

cessfully applied to materials science and chemistry to boost model performance.<sup>16,23</sup> We aim to extend this success to the catalysis domain, particularly to enhance the predictive capability of language-based models in adsorption energy prediction. Graph-assisted pretraining transfers the structural knowledge captured in graph embeddings to text embeddings in a self-supervised manner. This transfer of knowledge from a learned embedding space to the language model will help in our application of adsorption configuration energy predictions.

Additionally, we aim to show a potential use case of the Large Language Model (LLM) in making predictions without relying on precise atomic positions. For this, we use the generative capabilities of LLMs to generate desired textual input data for our predictive language model for energy prediction. Language models’ generative capabilities have recently shown success in structure generation for inorganic crystals.<sup>24,25</sup> In this study, we specifically fine-tune CrystaLLM to generate Crystallographic Information Files (CIFs) for relevant adsorbate-catalyst systems instead of inorganic crystals. Here, the fine-tuned CrystaLLM takes textual information about the chemical composition of the system, along with its surface orientation. Subsequently, we use the generated CIFs to derive the input string for our predictive language model. This method allows us to make energy predictions without knowing the full structure of the adsorbate-catalyst configurations.

## Results and discussion

### Framework

The language model-based approach for catalyst energy prediction leverages textual data for both training and inference. We have developed a multimodal pretraining framework, termed graph-assisted pretraining, to bridge the established graph-based approach with the newly introduced text-based approach within a shared latent space, as depicted in Figure 1. This method is introduced to enhance the accuracy of adsorption configuration energy predictions. This framework utilizes the CatBERTa model, which uses the RoBERTa encoder for text

processing and a linear regression header to predict catalyst system energies (see Figure 1 (b)).<sup>19</sup> Additionally, the EquiformerV2 model is employed as a graph encoder due to its capability in encoding structure (see Figure 1 (c)).<sup>9,26</sup> In this framework, both text and graph embeddings are utilized in a self-supervised manner during pretraining. Subsequently, the model undergoes a fine-tuning stage, where it is trained in a supervised manner using energy labels derived from DFT calculations. Importantly, the fine-tuning step relies exclusively on text input data, without the need for graph representations. More details can be found in the Methods section.

We conduct two types of downstream inference: one to assess the effect of graph-assisted pretraining and the other to demonstrate the model’s capability to predict energy without precise knowledge of the adsorbate-catalyst system structures. Both are depicted in Figure 2 (a). First, to evaluate the impact of graph-assisted pretraining on prediction accuracy, we made predictions on the test set strings derived from the ML-relaxed structure. The CatBERTa model, which takes textual strings as input, is trained using textual data derived from ML-relaxed structures to predict the energy of a relaxed configuration. Second, to demonstrate the model’s practicality in predicting energies without knowing the exact structures, we generate indicative structures in Crystallographic Information File (CIF) format using a large language model (LLM). This is done by providing the chemical composition and surface orientation of the adsorbate and catalyst as input. The generated CIFs are converted into textual strings compatible with CatBERTa input.

The textual strings are generated by converting structural information into a specific format containing three sections, as illustrated in the bottom box of Figure 2 (a). The first section represents the adsorbate’s chemical symbol, and the second part includes the catalyst’s chemical symbols and Miller index, indicating the chemical composition and surface orientation respectively. The final section describes the adsorption configuration, capturing the primary and secondary interacting atoms in the adsorbate and the top layers of the catalyst surface, identified using the Pymatgen library.<sup>27</sup> Further details on this structure-to-text

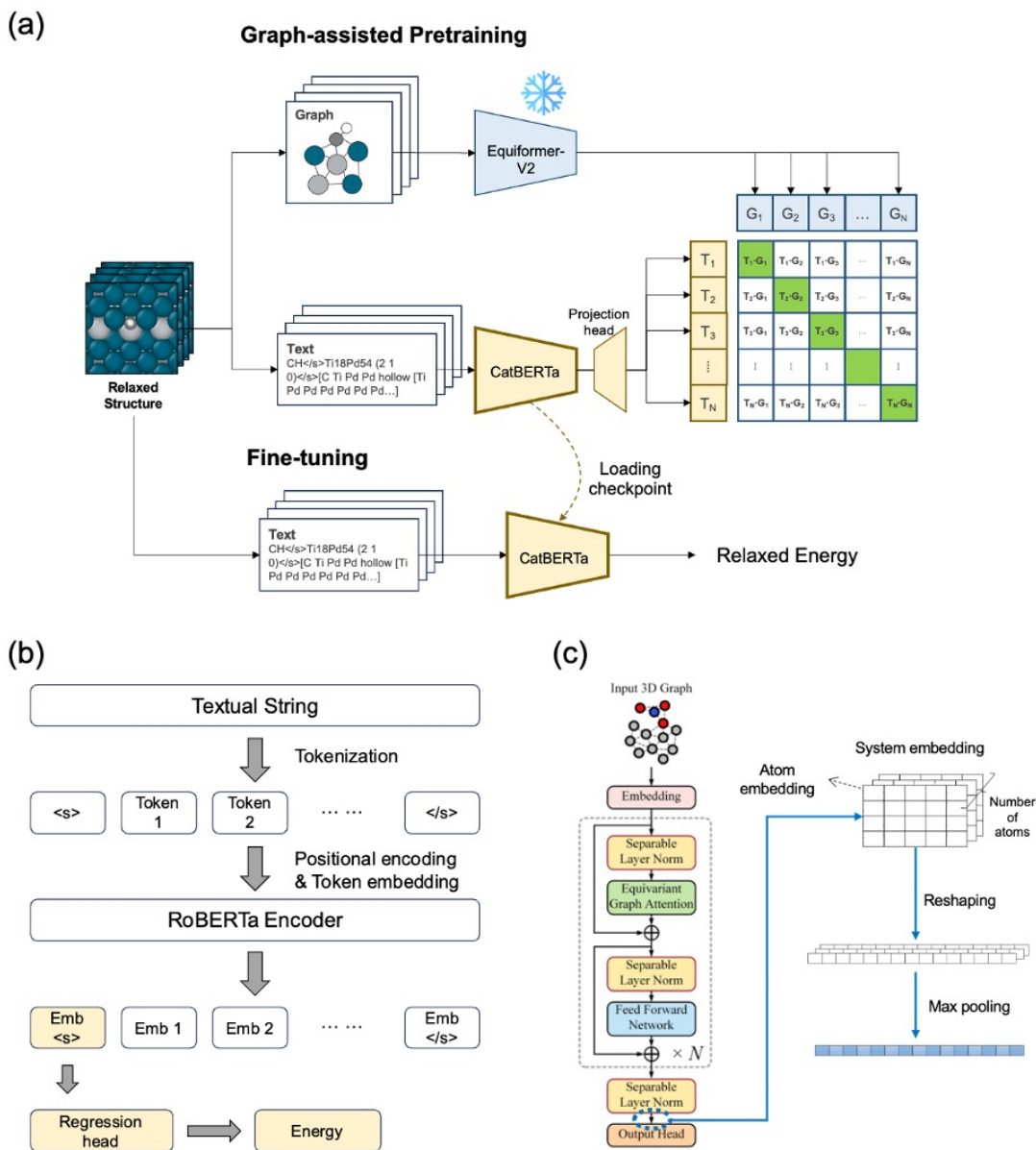


Figure 1: Overview of the model training framework. **a** The training process consists of two steps: graph-assisted pretraining and energy prediction fine-tuning. **b** The CatBERTa model is used as the text encoder. **c** The EquiformerV2 model serves as the graph encoder, and the graph embedding from the final layer is converted to a 1D format by reshaping and max pooling the collection of atom embeddings. The architecture image is taken from the original EquiformerV2 paper.<sup>26</sup>

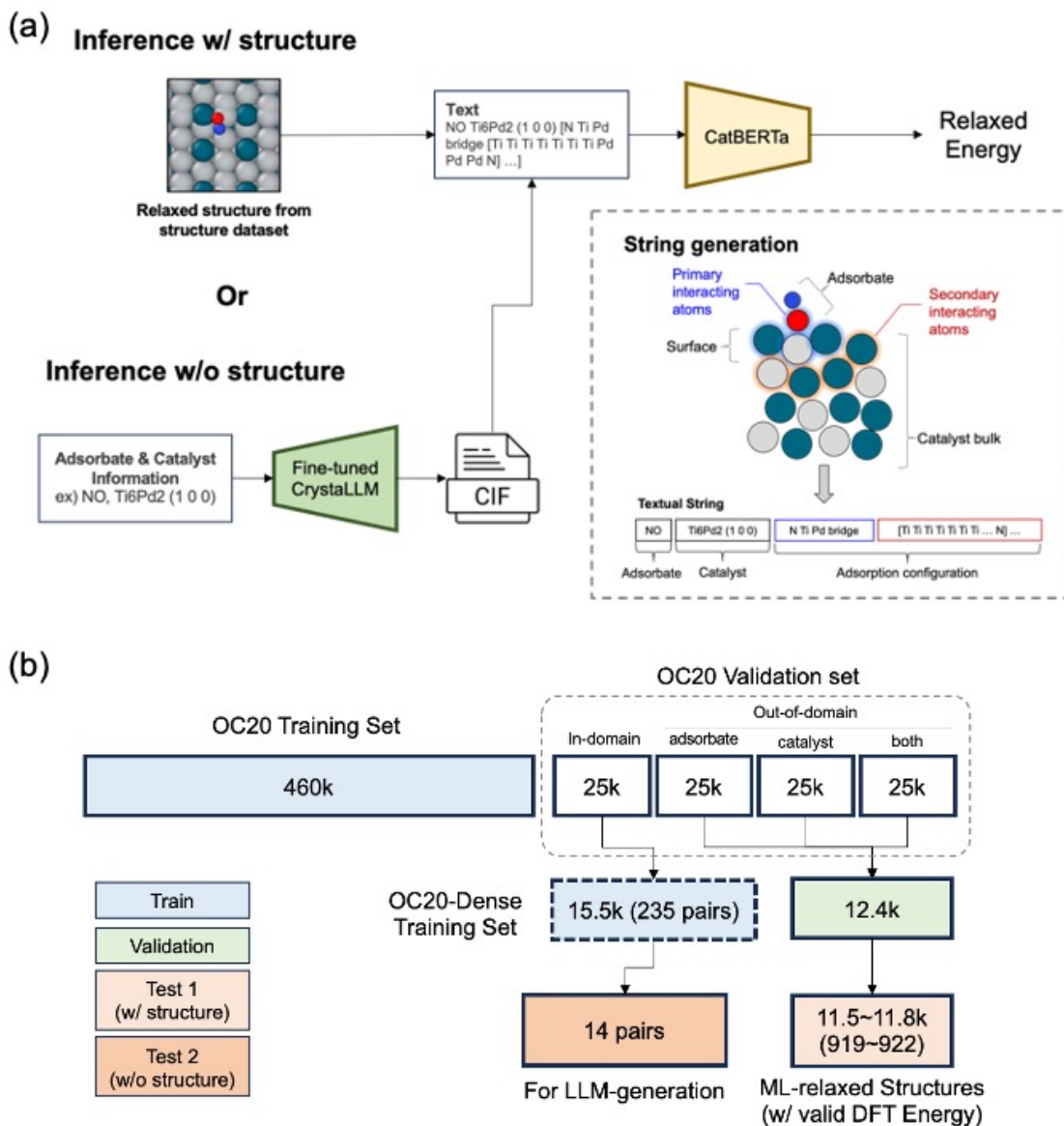


Figure 2: Model inference framework and data split. **a** Generated CIFs provide structure information, including atomic positions, types, and unit cell details. Both structure data and CIFs can be converted into textual strings compatible with CatBERTa input, following the string conversion logic shown in the bottom right box. **b** Dataset split for training, validation, and testing of CatBERTa involves DFT-relaxed structures stored in the OC20 and OC20-Dense datasets. We selected a subset of 14 adsorbate-catalyst pairs from 235 unique pairs in the OC20-Dense training dataset for inference on LLM-derived strings, not from the entire set of 15.5k configurations. These 14 pairs represent 875 configurations.

conversion process are available in the Methods section.

## Data pipeline

The textual string input for CatBERTa training is derived from the relaxed structures in the Open Catalyst 2020 (OC20) and Open Catalyst 2020 Dense (OC20-Dense) datasets. For both graph-assisted pretraining implementation and CrystaLLM fine-tuning, training and validation are conducted using texts sourced from DFT-relaxed structures. Specifically, for the first case, we convert the relaxed structures to string representations and use them for the training and validation process. For the latter case, we create CIFs for the relaxed structures, then use them for the training and validation process when fine-tuning CrystaLLM.

We have two types of inference, as illustrated in Figure 2 (a). In the first case of graph-assisted pretraining evaluation, predictions are made on strings generated from ML-relaxed structures. These ML-relaxed structures, along with their DFT-calculated energy labels, are provided by the Open Catalyst Project Challenge 2023.<sup>9</sup> GemNet-OC, SCN, and eSCN are used for the ML relaxation process. This process yields 11,508, 11,630, and 11,755 relaxed structures from each model, respectively, as shown in Figure 2 (b). To obtain valid DFT energies, DFT single-point calculations were performed on ML-relaxed structures. These were prepared by the dataset provider and included in the publicly available dataset. Our model’s accuracy is then evaluated using approximately 920 of these ML-relaxed structures with valid DFT energies. We quantify the uncertainty of our model’s predictions by calculating the standard deviation across predictions for structures relaxed using GemNet-OC, SCN, and eSCN. Their individual results are listed in Table S3. For embedding and attention score analysis, we use the entire set of ML-relaxed structures, ranging from 11,508 to 11,755, regardless of whether these structures have verified DFT energies.

For inference on the LLM-derived strings, predictions are made based on strings derived from adsorbate and catalyst information. The aim is to demonstrate the potential of generating plausible textual string representations using the LLM framework. As shown in Figure



2 (b), a subset of adsorbate and catalyst pair information is chosen from the original OC20-Dense training set, which contains 235 unique adsorbate-catalyst pairs. We extract the adsorbate, catalyst, and Miller index information from these pairs and use them as prompts for the fine-tuned CrystaLLM framework.

## Graph-assisted pretraining

Graph-assisted pretraining, a core component of our framework, is designed to transfer knowledge from graph embeddings to text embeddings. This approach bridges the gap between GNNs, which show great performance in energy and force predictions, and language models, which process human-interpretable data but do not take the entire structure as input. We select EquiformerV2 as the graph encoder due to its excellent performance with the OC20 dataset.<sup>26,28</sup> The CatBERTa model serves as the text encoder, producing text embeddings that are then projected to match the dimensions of the graph embeddings. To align these embeddings, we apply a contrastive loss to increase the similarity between embeddings from the same adsorbate-catalyst configurations, with the graph encoder remaining frozen.

Applying this method to the embedding space offers utility and flexibility. It operates solely on embeddings without downstream-task-specific labels, such as regression labels or classification categories. This means that we do not need to obtain labels for this pretraining stage. The downstream fine-tuning process can remain text-only, like the standard CatBERTa method. Once a properly pretrained checkpoint bridging graph and text modalities is established, it can be applied to multiple downstream tasks. Utilizing the embedding space also enhances generalizability, allowing the method to be applied to various encoders, provided their embedding sizes match. This graph-assisted pretraining method significantly improves prediction accuracy and adaptability across different datasets and tasks.

The graph-assisted pretraining method results in a substantial reduction in MAE, as shown in Table 1, with decreases ranging from 7.4% to 9.8%. To evaluate the enhancement from graph-assisted pretraining, we compare the prediction results of CatBERTa with and

without this pretraining method. In all cases, graph-assisted pretraining improves downstream prediction accuracy. Notably, pretraining with OC20 also benefits fine-tuning solely with OC20-Dense, despite there being no overlap between these datasets. This indicates that graph-assisted pretraining can serve as a transferable pretraining strategy, bridging the gap between high-performing GNNs and emerging Transformer-based language model approaches. It demonstrates the potential of self-supervised pretraining on one dataset to enhance performance on downstream tasks involving a different dataset. Prediction visualization and outlier analysis are provided in the supplementary information.

Table 1: Performance comparison of CatBERTa with and without graph-assisted pretraining (GAP). ‘‘Combined’’ refers to a combination of OC20 and OC20-Dense datasets.

	GAP Data (size)	Fine-tuning Data (size)	Prediction Results		Improvement from GAP	
			MAE [eV] ( $\downarrow$ )	$R^2$ [-] ( $\uparrow$ )	MAE (%) ( $\downarrow$ )	$R^2$ (%) ( $\uparrow$ )
CatBERTa	-	OC20 (460k)	$0.713 \pm 0.014$	$0.584 \pm 0.014$	-	-
	-	OC20-Dense (16k)	$0.542 \pm 0.011$	$0.712 \pm 0.008$	-	-
	-	Combined (476k)	$0.378 \pm 0.005$	$0.863 \pm 0.005$	-	-
GAP-CatBERTa	OC20 (460k)	OC20 (460k)	$0.643 \pm 0.020$	$0.691 \pm 0.015$	-9.82	+18.32
	OC20 (460k)	OC20-Dense (16k)	$0.502 \pm 0.010$	$0.764 \pm 0.008$	-7.38	+7.30
	Combined (476k)	Combined (476k)	$0.346 \pm 0.005$	$0.882 \pm 0.002$	-8.47	+2.20

Additionally, the incorporation of OC20-Dense highlights the importance of model exposure to diverse adsorption configurations. Although the OC20-Dense training dataset is only 3.5% the size of the OC20 training dataset, it significantly contributes to energy prediction accuracy. Fine-tuning solely with OC20-Dense results in a 24% smaller MAE compared to fine-tuning with OC20. Furthermore, adding OC20-Dense to the fine-tuning process reduces the MAE by approximately 51.5%. The test set, consisting of ML-relaxed structures from OC20-Dense, exhibits configurational diversity. Thus, greater exposure to diverse configurations during pretraining leads to improved prediction accuracy.

## Enhancement in the latent space and attention score

As graph-assisted pretraining is applied to the embeddings, it is essential to examine the latent space to observe its effects. Graph-assisted pretraining can align the graph and text

embeddings from the same adsorbate-catalyst configurations. Figure 3 (a) and (b) show the similarity matrix of graph and text embeddings. After applying graph-assisted pretraining, a clear diagonal line appears in the similarity matrix, indicating the alignment between embeddings in the latent space.

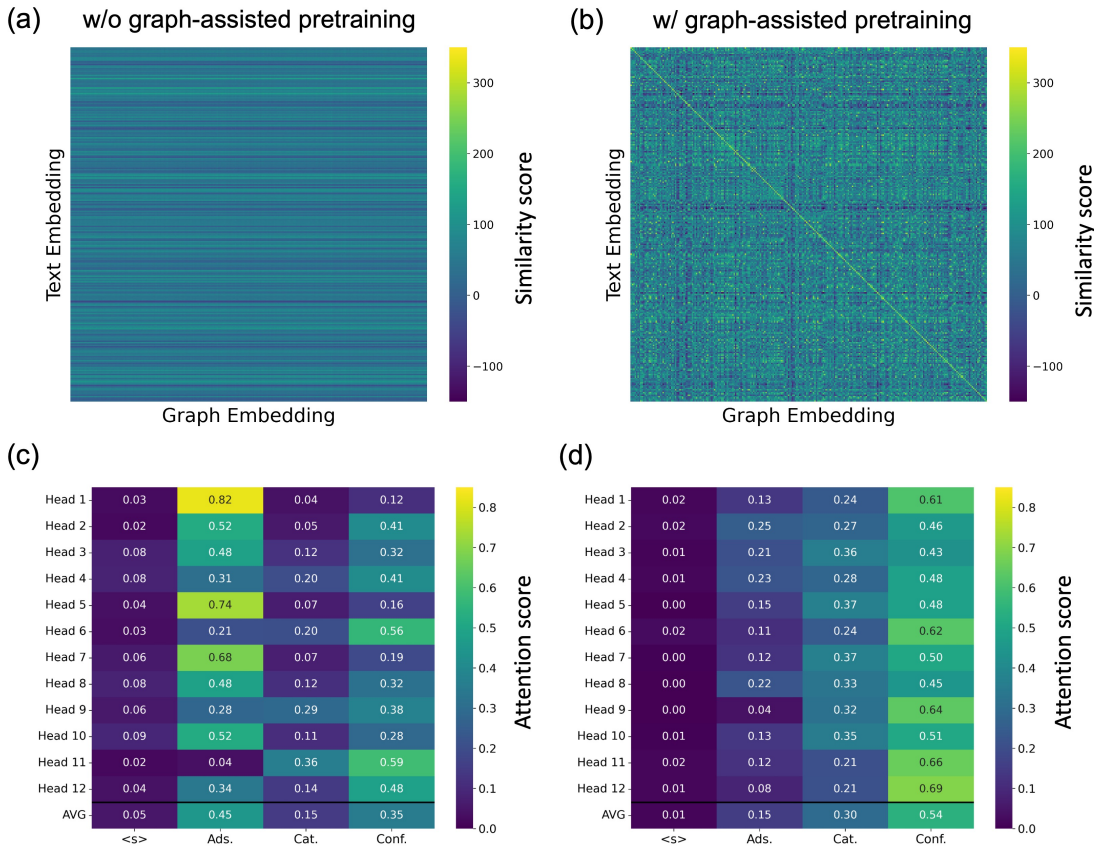


Figure 3: Analysis of similarity scores and sectional attention with and without graph-assisted pretraining. **a** and **b** displays similarity score analysis. **c** and **d** shows sectional attention score comparison. The left panels are without graph-assisted pretraining, while the right panels are with it. These results are derived from model predictions, which were trained on the OC20 dataset and evaluated using text strings from the GemNet-OC-relaxed structures.

Figure 3 (a) and (b) show the similarity matrices of graph and text embeddings. After applying graph-assisted pretraining, a clear diagonal line appears, indicating the alignment between embeddings in the latent space. By comparing the left and right panels, we can clearly observe that the similarity score of actual pairs becomes higher than that of random pairs, which are not supposed to have correlations. The horizontal stripes in the similarity

matrix before applying graph-assisted pretraining are due to the weight initialization in the final layer of EquiformerV2.

The analysis of attention scores in the final layer provides insights into how the model allocates attention. Our input string consists of three sections as discussed earlier, and the section-wise attention scores reveal the model’s focus on each section. We extract and average the attention scores for the “<s>” token, which is fed to the regression head, across three distinct sections: the adsorbate, the catalyst, and the adsorption configuration. Additionally, we compute the attention score of the “<s>” token with respect to itself. The section-wise averaged attention scores are presented in Figure 3 (c) and (d).

Graph-assisted pretraining makes the model focus more on the adsorption configuration section. This attention redirection occurs across all 12 attention heads. Specifically, while the vanilla CatBERTa model primarily concentrates on the adsorbate section, the graph-assisted pretraining reallocates the model’s focus towards both the catalyst and configuration sections. This shift in attention aligns with the physical principle that the interaction of the adsorbate with the catalytic surface as a whole is more critical than analyzing the adsorbate and the surface as separate entities.<sup>29,30</sup>

## Energy prediction for unknown structures

The ideal benefit of using language models and language representations is to bypass the need for atomic structures. However, the current textual string input for the CatBERTa model still requires neighbor atom information. To address this, we explore using an LLM to generate the necessary input data solely based on adsorbate and catalyst information. The main idea is to derive the last configuration section from the first two sections, which pertain to the adsorbate and catalyst details (refer to Figure 2 (a)).

For this purpose, we use CrystaLLM, which was originally trained to generate CIFs of inorganic crystals.<sup>24</sup> We fine-tune the pretrained CrystaLLM using CIFs from relaxed structures in the Open Catalyst training datasets, as illustrated in Figure 4. CrystaLLM

autoregressively predicts the next tokens in the CIF until it encounters two consecutive ‘\n’ tokens. The initial prompt to the CrystaLLM is set as the first two parts of the CatBERTa input string, which includes adsorbate and catalyst information along with the Miller index. These first two parts of the CatBERTa input string are derived from the metadata of the Open Catalyst dataset,<sup>3,8</sup> encompassing the adsorbate chemical symbol, catalyst chemical symbol, and Miller index—information that relies on atomic geometry and is experimentally obtainable.

As the model autoregressively generates the next token based on the given tokens, the model completes the rest of the CIF from the given starting prompt. For example, the input for the fine-tuned CrystaLLM might be ‘data\_CCH3</s>Al12As12 (1 1 1)’, and the output from the model would be the corresponding CIF file, which contains indicative structure information. “Indicative” means that, while the generated CIFs do not necessarily guarantee validity, they can contain some degree of information about the structures (see Figure 4 (c)).

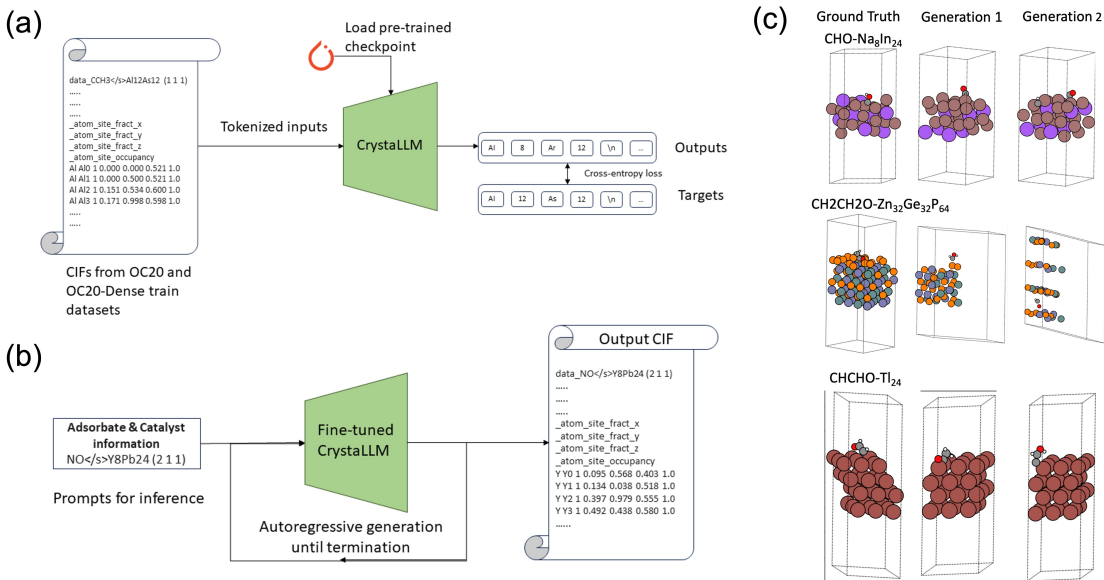


Figure 4: CrystaLLM framework. **a** illustrates the fine-tuning step using the CIFs from the relaxed structures in the OC20 and OC20-Dense training datasets. **b** depicts the inference process using the provided adsorbate and catalyst pair information. **c** shows visualization examples. These systems are from the OC20 validation set.

For =unknown structure systems, we can use the proposed generative language model

approach along with the predictive CatBERTa model to obtain energy predictions. From the OC20-Dense training dataset, which contains 235 unique adsorbate-catalyst pairs, we downsampled 14 pairs based on the type and number of elements in the adsorbate and catalyst bulk. These selected pairs of adsorbate and catalyst information are used as starting prompts, which are fed into the fine-tuned CrystaLLM to generate CIFs (see Figure 4 (b)). We iterated through three generations and selected the CIFs where the composition of generated atoms matched the given adsorbate and catalyst chemical symbols within a certain threshold. The detailed process is provided in the Methods section. These CIFs are then converted into textual string inputs for CatBERTa prediction. Each adsorbate-catalyst pair can have multiple adsorption configurations in the OC20-Dense dataset. Even though we downsampled to 14 adsorbate-catalyst pairs, the number of their total adsorption configurations is 875.

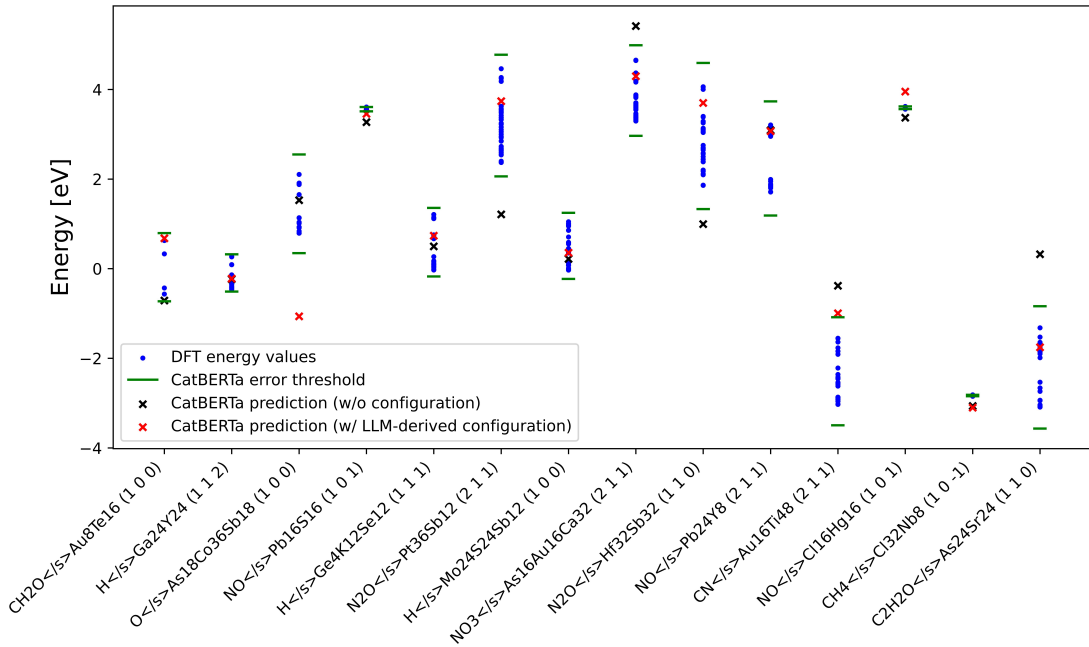


Figure 5: Validation of LLM-derived strings as input for the CatBERTa model. Blue dots represent the energy of different adsorption configurations for each adsorbate-catalyst pair. The number of adsorption configurations ranges from 4 to 130, with a mean value of 62.5.

We benchmark the energy predictions using these adsorbate-catalyst pairs to determine if

the LLM-derived configuration strings can help the energy prediction. For this, we compared two types of predictions; one is made only with the adsorbate and catalyst section, while the other is made on the strings including LLM-derived configuration strings. Subsequently, we compare those predicted values with the actual DFT energy values of possible adsorption configurations for those chosen adsorbate-catalyst pairs in the OC20-Dense dataset, as shown in Figure 5. This comparison allows us to evaluate whether the predictions on the LLM-derived strings fall within the actual range of DFT energies across possible configurations and whether the addition of LLM-derived configuration strings can enhance the possibility. For this prediction, we used CatBERTa, pretrained and fine-tuned with the OC20 dataset, making these predictions entirely out-of-domain since the adsorbate-catalyst pairs are from the OC20-Dense dataset.

In Figure 5, the blue points represent the DFT-calculated energy values for various adsorption configurations of each adsorbate-catalyst pair. The range of blue points indicates the potential variations in adsorption configurations for each pair. The red X marks represent CatBERTa predictions with LLM-derived configurations, while the black X marks represent predictions without them. The green lines above and below the blue points indicate CatBERTa’s intrinsic error threshold, with an average value of 0.24 eV. This threshold for each adsorbate-catalyst combination is derived from the standard deviation of CatBERTa’s predictions on the actual strings of those adsorption configurations, corresponding to the blue points. We add this value to the minimum and subtract it from the maximum values of the blue points, respectively, to establish the error threshold.

The results show that CatBERTa’s predictions with the LLM-derived configuration strings fall within the actual DFT energy ranges for 8 out of 14 pairs, while predictions without the LLM-derived configuration strings are valid for 5 out of 14 pairs. Additionally, when considering the DFT + CatBERTa error threshold, predictions with LLM-derived configurations fall within the range for 9 out of 14 pairs, compared to 6 out of 14 pairs without them, indicating an improvement. Thus, adding the configuration strings derived from the LLM

framework improves prediction accuracy, a trend also supported by the MAE comparison.

## Conclusion

The recent adoption of language models in predicting material properties shows the potential of bypassing the exact atomic position of the systems. In the catalysis domain, the predictive language model, CatBERTa, enables a more seamless integration of features into the input data. Nonetheless, the current CatBERTa model shows a limitation in accurately distinguishing subtle energy variations across adsorption configurations. To effectively apply language models to predictive tasks in computational catalysis, it is essential to enhance the accuracy of these predictions. For this, we have introduced a multimodal pretraining approach, by integrating the graph and text embeddings in the latent space.

Our graph-assisted pretraining method enhances the accuracy of the language model by guiding the text modality with a graph modality. This method results in a 7.4-9.8% reduction in MAE compared to the prediction case without the graph-assisted pretraining. Additionally, the model pretrained with the OC20 dataset can also help improve prediction accuracy when fine-tuned with the OC20-Dense dataset, demonstrating its applicability across different datasets. This implies that building a solid pretrained checkpoint can enhance targeted downstream tasks. The key to accuracy improvement lies in making the fine-tuning step start with a more informed and aligned latent space.

Additionally, we leverage the autoregressive generative capabilities of the language model to enable energy prediction without knowing the precise atomic structure. We propose a method using a large language model as an input string data generator. Specifically, we integrate the fine-tuned CrystaLLM, which can generate indicative structures in CIF format. This approach allows us to generate textual input strings for the predictive CatBERTa model, based solely on the chemical composition or surface orientation. Therefore, we can make energy predictions for adsorbate-catalyst systems by only knowing the chemical compo-



sition and surface orientation. This demonstrates the potential of using a language model as a comprehensive framework for energy prediction when exact atomic positions are unattainable.

## Methods

### Open Catalyst dataset

The OC20 dataset stands as the most extensive and varied dataset for heterogeneous catalysts. It encompasses over 1.2 million DFT relaxations, all using the revised Perdew-Burke-Emzerhof (RPBE) functional.<sup>3,31</sup> This dataset features various tasks, including Initial-Structure-to-Energy (IS2RE), Initial-Structure-to-Relaxed-Structure (IS2RS), and Structure-to-Energy-and-Force (S2EF). In our study, we focus on the data for the IS2RE/IS2RS task, which consists of 460,328 DFT relaxations. Our objective is to predict the relaxed energy of each adsorbate-catalyst configuration based on its final relaxed structure, leading us to specifically select the last frame of these relaxation trajectories.

To investigate the global minimum energy, also known as the adsorption energy, of adsorbate-catalyst pairs, the OC20-Dense dataset was developed.<sup>8</sup> The OC20 dataset, while extensive in types of adsorbates and catalytic surfaces, lacks variation in adsorption configurations. OC20-Dense dataset addresses this by densely enumerating these configurations. The initial configurations of adsorbates on surfaces are produced using both heuristic and random approaches.<sup>8,27,32</sup> These configurations then undergo relaxations using both ML and DFT methods. The OC20-Dense dataset contains 995 distinct adsorbate-catalyst pairs, evenly selected from the in-domain and three out-of-domain splits, from the OC20 validation set (see Figure 2). Our training and validation data splits conform to the dataset provided by the Open Catalyst Challenge 2023.<sup>9</sup> The training set for OC20-Dense, drawn from the in-domain split of the OC20 validation set, comprises 15,450 data entries and serves as an optional addition. The validation set for the OC20-Dense is created by randomly selecting

12,372 data entries from its three out-of-domain splits.

## **GNN-relaxed structures**

As part of the Open Catalyst Challenge 2023, the Open Catalyst Project has provided a set of ML-relaxed structures along with their energies calculated using DFT. These structures, originating from the OC20-Dense validation set and illustrated in Figure 2 (b), were relaxed using models like GemNet-OC, SCN, and eSCN. Any relaxed structures that are invalid or lack valid DFT energy values were excluded by the dataset creator.<sup>8,9</sup> This includes cases where the adsorbate fails to bind to the surface, decomposes into different atoms or molecules, or causes significant alterations to the surface from its original state. After filtering out these invalid configurations, the remaining counts for the ML-relaxed test sets using the GemNet-OC, SCN, and eSCN models are 11,508, 11,630, and 11,755 structures, respectively. Within these datasets, only a subset of structures—919, 922, and 922 respectively—have valid DFT-verified energy values. Our accuracy analysis concentrates on these approximately 920 ML-relaxed structures, each supported by a reliable DFT energy assessment. Meanwhile, the embedding and attention score analyses fully utilize predictions on all the valid ML-relaxed structures.

## **Structure-string conversion**

The input data is entirely text-based, adhering to the string-type input format outlined in the original CatBERTa paper.<sup>19</sup> We generate textual strings by converting the relaxed structures in the OC20 and OC20-Dense datasets, as illustrated in Figure 2. Our textual input format is structured into three segments: the adsorbate, the catalytic surface, and the depiction of the adsorption configuration. Specifically, the adsorbate segment simply contains its elemental symbol. For the catalytic surface part, we integrate information about the catalyst’s overall composition along with its Miller index. For these two segments, the information is sourced from the pre-existing metadata of the OC20 dataset. The depiction

of the adsorption configuration is achieved by pinpointing both the primary and secondary atoms involved in the interaction. This method is selected due to its proven effectiveness in predicting energy outcomes in previous research.<sup>19</sup> In this process, we identify these interacting elements using the Pymatgen library. First, we establish atomic connectivity based on a predefined cutoff radius, which is a covalent radius of the atom. Then, we pinpoint the atoms connected to those in the adsorbate and surface. The connected atoms of the adsorbate atoms are classified as primary interacting atoms, while the neighboring atoms of the primary interacting atoms on the surface are grouped as secondary interacting atoms.

To convert structures from LLM-generated CIFs, we employ a more lenient and simplified approach. Initially, we identify and specify only the adsorbate atom closest to the surface. Next, we gather the primary neighbor atoms surrounding this adsorbate atom. Following this, we collect the secondary neighbor atoms from the primary neighbors. In this process, we use a multiplier of 4 for the cut-off radius, meaning the neighbor atoms are those within four times the covalent radius. This approach is based on the understanding that the structures in the generated CIF are indicative, not exact.

## CatBERTa

In this research, we employ the CatBERTa model as a predictive language model. This text-based model is specifically designed and trained for predicting relaxed energy in adsorbate-catalyst systems. The model incorporates the RoBERTa encoder, originally pretrained on an extensive natural language corpus that includes resources such as BookCorpus and English Wikipedia, cumulatively exceeding 160GB.<sup>33</sup> The RoBERTa, diverging from the conventional BERT model<sup>34</sup> which masks a fixed 15% of tokens in each epoch during training, adopts a dynamic masking approach. This method alters the masked tokens variably across different training epochs, thereby improving the model’s proficiency in predicting masked words and grasping syntactic and semantic nuances.

The CatBERTa model is fine-tuned for an energy prediction task. The original RoBERTa’s

classification head is replaced with a regression head, comprising a linear and activation layer. This modification allows CatBERTa to generate a singular scalar value of energy predictions. For this prediction, the embedding of the special “<s>” token, after encoder processing, serves as input for this regression head. The training hyperparameters and the architecture details of the CatBERTa model are provided in Table S1, while pretraining and fine-tuning strategies are listed in Table S2.

## EquiformerV2

The Equiformer is a GNN which is SE(3)/E(3)-equivariant, adeptly fusing the inductive biases of equivariance with the dynamic strengths of Transformers.<sup>28</sup> The Equiformer stands out by demonstrating that Transformers can be effectively adapted to 3D atomistic graphs. This is achieved by two main factors. First, the Equiformer modifies the traditional Transformer by substituting SE(3)/E(3)-equivariant operations for the original operations. Second, the Equiformer model introduces equivariant graph attention, a novel attention mechanism.

In the pretraining stage, we utilize the EquiformerV2 embedding for graph representation purposes due to its excellent performance in the OC20 dataset. The EquiformerV2,<sup>26</sup> a refined version of the original Equiformer, brings to the table a host of enhancements. These improvements encompass the replacement of SO(3) convolutions with eSCN convolutions, the introduction of attention re-normalization, the incorporation of separable S2 activation, and the application of separable layer normalization.<sup>26</sup> Such advancements have elevated the EquiformerV2, especially in the task of energy and force predictions on the OC20 dataset. The model demonstrates state-of-the-art accuracy in its performance, achieving an MAE of 0.22 eV for the S2EF task and 0.31 eV for the IS2RE task, outperforming other benchmarked models.

The graph embeddings in our case, are extracted after the final layer normalization in the EquiformerV2 model, which precedes the energy and force prediction stage, as illustrated

in Figure 1 (c). Within this model, each atom is represented as a node, and each atom node is characterized by a two-dimensional embedding tensor, collectively forming a three-dimensional tensor for the entire system. The size of the system tensor is defined by the number of atoms, the count of spherical channels, and the maximum degree of spherical harmonics involved.<sup>26</sup> The extraction of graph embeddings begins with reshaping the two-dimensional atom embedding tensor into a one-dimensional tensor. Subsequently, max-pooling is applied across all these one-dimensional atom embeddings in the system, yielding a single, comprehensive embedding for each system. In our study, the final embedding of each system is represented by a tensor with a size of 3,200. Consequently, during the graph-assisted pretraining phase, text embeddings, initially sized at 768, undergo a linear projection head to match the 3,200-size tensor.

## Contrastive loss

Graph-assisted pretraining synergistically aligns text and graph embeddings through a self-supervised framework. Utilizing the graph encoder EquiformerV2 in a static (frozen) state, this method is specifically designed to transfer the insights from the graph to the text modality.

Inspired by the methodology used in Contrastive Language-Image Pretraining (CLIP),<sup>35</sup> the graph-assisted pretraining strategy incorporates both text and graph encoders. The pretraining mechanism is centered around the optimization of a symmetric cross-entropy loss.<sup>36</sup> This optimization process aims to increase the similarity between embeddings from matching text-graph pairs while decreasing the similarity between those from unmatching pairs. By using a contrastive loss function, the primary objective is to establish a meaningful correlation between text and graph embeddings. The overarching goal is to precisely align embeddings from corresponding text-graph pairs while effectively differentiating between non-corresponding pairs.

The mathematical formulation of the loss function is defined as follows:

$$L = -\frac{1}{N} \sum_{i=1}^N \log \frac{e^{\text{sim}(I_i, T_i)/\tau}}{\sum_{j=1}^N e^{\text{sim}(I_i, T_j)/\tau} \mathbb{I}_{\{i \neq j\}}} - \frac{1}{N} \sum_{i=1}^N \log \frac{e^{\text{sim}(T_i, I_i)/\tau}}{\sum_{j=1}^N e^{\text{sim}(T_i, I_j)/\tau} \mathbb{I}_{\{i \neq j\}}} \quad (1)$$

In this expression,  $T_i$  and  $G_i$  represent the embeddings of the  $i$ -th text and graph, respectively. The function  $\text{sim}(G_i, T_j)$  calculates the cosine similarity between the embeddings of the  $i$ -th graph and  $j$ -th text. Additionally,  $\tau$  is introduced as a temperature parameter, serving to appropriately scale the similarity scores within the model.

## Fine-tuning CrystaLLM

CrystaLLM is a GPT-2-based large language model designed to generate crystal structures in CIF format for a given composition and, optionally, a specified space group.<sup>24,37</sup> Adapted from the nanoGPT<sup>38</sup> model implementation, this framework has been trained from scratch with a vocabulary size of 371, specifically for inorganic crystal systems. The training data was sourced from various databases, including the Materials Project,<sup>39</sup> the Open Quantum Materials Database,<sup>40</sup> and NOMAD.<sup>41</sup> The tokenizers for the CrystaLLM operates on character bytes instead of words. The CrystaLLM (large) model, which we use in our analysis as our pretrained framework, consists of 16 layers with 16 heads each, and individual block sizes of 2,048. This model has been trained for 48,000 epochs, enabling it to predict text-based structural CIF representations of various crystal systems by leveraging the generative capabilities of language models.

By fine-tuning the pretrained model over the combined training data from the OC20 and OC20-Dense datasets for 6,000 epochs, we leverage the learned embedding space of the existing model. This allows us to transfer the corresponding knowledge to our specific task. The fine-tuning learning rate is set to 6e-4, compared to the pretraining learning rate of 1e-3, to further enhance the model’s generalization capabilities. Consequently, our fine-tuned CrystaLLM generates CIFs for target adsorbate-catalyst systems using only the adsorbate and catalyst bulk chemical symbols, along with surface orientation.

## CrystaLLM subsampling

In this study, we applied targeted selection criteria to extract relevant adsorbates and catalysts from the OC20-Dense training dataset. The main reason for this is to adhere to the token length constraints of our tokenizer, which is set at 3,000. Additionally, as the original model’s generative performance has not been universally validated, we focused on a simplified subset to understand potential use cases.

We selected systems from the OC20-Dense dataset where the adsorbates contain no more than five atoms each, across 51 unique adsorbates. Notably, each adsorbate is composed of a maximum of three different types of elements, resulting in a total of 27 unique, filtered adsorbates. To comply with the tokenizer’s maximum token length, we also imposed a constraint on the total number of atoms in the catalyst system. Specifically, we selected catalyst systems with a total atom count not exceeding 72. Applying these filters to the OC20-Dense training dataset yielded 108 unique adsorbate-catalyst pairs out of 235 pairs.

From these 108 adsorbate-catalyst pairs, we randomly selected 14 systems that could keep the total number of adsorption configurations under 1,000 for ease of inference. The adsorbate and catalyst information from these systems was used as prompts for inference within the CrystaLLM framework. The fine-tuned CrystaLLM generated three CIF files for each adsorbate-catalyst combination. These generated CIFs underwent a validation process to account for the stochastic nature of the language model, ensuring that only entries meeting specified criteria for the number and type of elements and atoms were included. This criterion required that the generated CIF’s adsorbate be an exact match with the prompt and that the generated catalyst’s atom count be within a 12-atom error threshold relative to the prompt catalyst system. This tolerance level was established to accommodate minor discrepancies while ensuring robust validation without excluding valid entries due to minor variations.

Following this validation process, all the CIF files that passed the criteria were converted into the desired string configurations. If more than one generation out of three passed the criteria for each pair, we randomly selected one CIF. The overall filtering process resulted in

14 unique adsorbate-catalyst pairs. This subset serves to evaluate our proposed framework. It is noteworthy that these 14 adsorbate-catalyst systems correspond to 875 overall configurations in the original training dataset, providing a total of 875 DFT-calculated energy values.

## Supporting Information Available

Hyperparameters and architecture of CatBERTa, Pretraining and Fine-tuning, Alignment in latent space, Results from diverse ML-relaxed structures, Prediction visualization, Prediction results of duplicate text sets

## Technology Use Disclosure

ChatGPT was used to help prepare the preprint version of this manuscript, specifically for grammar and typo corrections. All information in this manuscript has been read, corrected, and verified by all authors.

## Data Availability Statement

Access to the Open Catalyst 2020 dataset is provided via this link: <https://github.com/FAIR-Chem/fairchem>. The Open Catalyst 2020 Dense dataset and relevant data about the Open Catalyst Challenge 2023 are available at: <https://github.com/Open-Catalyst-Project/AdsorbML>.

## Code Availability Statement

The Python code employed in this study is available on GitHub at the following link: <https://github.com/hoon-ock/multi-view>.



## References

- (1) Behler, J. Perspective: Machine learning potentials for atomistic simulations. *The Journal of Chemical Physics* **2016**, *145*, 170901.
- (2) Zitnick, C. L. et al. An Introduction to Electrocatalyst Design using Machine Learning for Renewable Energy Storage. 2020; <https://arxiv.org/abs/2010.09435>.
- (3) Chanussot, L. et al. Open Catalyst 2020 (OC20) Dataset and Community Challenges. *ACS Catalysis* **2021**, *11*, 6059–6072.
- (4) Reiser, P.; Neubert, M.; Eberhard, A.; Torresi, L.; Zhou, C.; Shao, C.; Metni, H.; van Hoesel, C.; Schopmans, H.; Sommer, T.; Friederich, P. Graph neural networks for materials science and chemistry. *Communications Materials* **2022**, *3*, 93.
- (5) Goldsmith, B. R.; Esterhuizen, J.; Liu, J.-X.; Bartel, C. J.; Sutton, C. Machine Learning for Heterogeneous Catalyst Design and Discovery. *AIChE Journal* **2018**, *64*, 2311–2323.
- (6) Wander, B.; Broderick, K.; Ulissi, Z. W. Catlas: an automated framework for catalyst discovery demonstrated for direct syngas conversion. *Catal. Sci. Technol.* **2022**, *12*, 6256–6267.
- (7) Tran, R.; Wang, D.; Kingsbury, R.; Palizhati, A.; Persson, K. A.; Jain, A.; Ulissi, Z. W. Screening of bimetallic electrocatalysts for water purification with machine learning. *The Journal of Chemical Physics* **2022**, *157*, 074102.
- (8) Lan, J.; Palizhati, A.; Shuaibi, M.; Wood, B. M.; Wander, B.; Das, A.; Uyttendaele, M.; Zitnick, C. L.; Ulissi, Z. W. AdsorbML: a leap in efficiency for adsorption energy calculations using generalizable machine learning potentials. *npj Computational Materials* **2023**, *9*, 172.
- (9) Open Catalyst Challenge. <https://opencatalystproject.org/challenge.html>, 2023; Accessed: December 24, 2023.

- (10) Xie, T.; Grossman, J. C. Crystal Graph Convolutional Neural Networks for an Accurate and Interpretable Prediction of Material Properties. *Phys. Rev. Lett.* **2018**, *120*, 145301.
- (11) Schütt, K. T.; Kindermans, P.-J.; Sauceda, H. E.; Chmiela, S.; Tkatchenko, A.; Müller, K.-R. SchNet: A continuous-filter convolutional neural network for modeling quantum interactions. 2017; <https://arxiv.org/abs/1706.08566>.
- (12) Gasteiger, J.; Shuaibi, M.; Sriram, A.; Günnemann, S.; Ulissi, Z.; Zitnick, C. L.; Das, A. GemNet-OC: Developing Graph Neural Networks for Large and Diverse Molecular Simulation Datasets. 2022; <https://arxiv.org/abs/2204.02782>.
- (13) Pablo-García, S.; Morandi, S.; Vargas-Hernández, R. A.; Jorner, K.; Žarko Ivković; López, N.; Aspuru-Guzik, A. Fast evaluation of the adsorption energy of organic molecules on metals via graph neural networks. *Nature Computational Science* **2023**, *3*, 433–442.
- (14) Studt, F. Grand Challenges in Computational Catalysis. *Frontiers in Catalysis* **2021**, *1*.
- (15) Giulimondi, V.; Mitchell, S.; Pérez-Ramírez, J. Challenges and Opportunities in Engineering the Electronic Structure of Single-Atom Catalysts. *ACS Catalysis* **2023**, *13*, 2981–2997.
- (16) Cao, Z.; Magar, R.; Wang, Y.; Barati Farimani, A. MOFormer: Self-Supervised Transformer Model for Metal–Organic Framework Property Prediction. *Journal of the American Chemical Society* **2023**, *145*, 2958–2967.
- (17) Balaji, S.; Magar, R. GPT-MolBERTa: GPT Molecular Features Language Model for molecular property prediction. 2023; <https://arxiv.org/abs/2310.03030>.
- (18) Xu, C.; Wang, Y.; Barati Farimani, A. TransPolymer: a Transformer-based language model for polymer property predictions. *npj Computational Materials* **2023**, *9*, 64.

- (19) Ock, J.; Guntuboina, C.; Barati Farimani, A. Catalyst Energy Prediction with CatBERTa: Unveiling Feature Exploration Strategies through Large Language Models. *ACS Catalysis* **2023**, *13*, 16032–16044.
- (20) Wang, S.; Temel, B.; Shen, J.; Jones, G.; Grabow, L. C.; Studt, F.; Bligaard, T.; Abild-Pedersen, F.; Christensen, C. H.; Nørskov, J. K. Universal Brønsted-Evans-Polanyi Relations for C–C, C–O, C–N, N–O, N–N, and O–O Dissociation Reactions. *Catalysis Letters* **2011**, *141*, 370–373.
- (21) Sutton, J. E.; Vlachos, D. G. A Theoretical and Computational Analysis of Linear Free Energy Relations for the Estimation of Activation Energies. *ACS Catalysis* **2012**, *2*, 1624–1634.
- (22) Ock, J.; Tian, T.; Kitchin, J.; Ulissi, Z. Beyond independent error assumptions in large GNN atomistic models. *The Journal of Chemical Physics* **2023**, *158*, 214702.
- (23) Huang, H.; Barati Farimani, A. Multimodal learning of heat capacity based on transformers and crystallography pretraining. *Journal of Applied Physics* **2024**, *135*, 165104.
- (24) Antunes, L. M.; Butler, K. T.; Grau-Crespo, R. Crystal Structure Generation with Autoregressive Large Language Modeling. 2024; <https://arxiv.org/abs/2307.04340>.
- (25) Gruver, N.; Sriram, A.; Madotto, A.; Wilson, A. G.; Zitnick, C. L.; Ulissi, Z. Fine-Tuned Language Models Generate Stable Inorganic Materials as Text. 2024; <https://arxiv.org/abs/2402.04379>.
- (26) Liao, Y.-L.; Wood, B.; Das, A.; Smidt, T. EquiformerV2: Improved Equivariant Transformer for Scaling to Higher-Degree Representations. 2023; <https://arxiv.org/abs/2306.12059>.
- (27) Ong, S. P.; Richards, W. D.; Jain, A.; Hautier, G.; Kocher, M.; Cholia, S.; Gunter, D.; Chevrier, V. L.; Persson, K. A.; Ceder, G. Python Materials Genomics (Pymatgen): A

- Robust, Open-source Python Library for Materials Analysis. *Computational Materials Science* **2013**, *68*, 314–319.
- (28) Liao, Y.-L.; Smidt, T. Equiformer: Equivariant Graph Attention Transformer for 3D Atomistic Graphs. 2023; <https://arxiv.org/abs/2206.11990>.
- (29) Gao, W.; Chen, Y.; Li, B.; Liu, S.-P.; Liu, X.; Jiang, Q. Determining the adsorption energies of small molecules with the intrinsic properties of adsorbates and substrates. *Nature Communications* **2020**, *11*, 1196.
- (30) Esterhuizen, J. A.; Goldsmith, B. R.; Linic, S. Theory-Guided Machine Learning Finds Geometric Structure-Property Relationships for Chemisorption on Subsurface Alloys. *Chem* **2020**, *6*, 3100–3117.
- (31) Hammer, B.; Hansen, L. B.; Nørskov, J. K. Improved Adsorption Energetics within Density-Functional Theory using Revised Perdew-Burke-Ernzerhof Functionals. *Phys. Rev. B* **1999**, *59*, 7413–7421.
- (32) Boes, J. R.; Mamun, O.; Winther, K.; Bligaard, T. Graph Theory Approach to High-Throughput Surface Adsorption Structure Generation. *The Journal of Physical Chemistry A* **2019**, *123*, 2281–2285.
- (33) Liu, Y.; Ott, M.; Goyal, N.; Du, J.; Joshi, M.; Chen, D.; Levy, O.; Lewis, M.; Zettlemoyer, L.; Stoyanov, V. RoBERTa: A Robustly Optimized BERT Pretraining Approach. 2019; <https://arxiv.org/abs/1907.11692>.
- (34) Devlin, J.; Chang, M.-W.; Lee, K.; Toutanova, K. BERT: Pre-training of Deep Bidirectional Transformers for Language Understanding. 2019; <https://arxiv.org/abs/1810.04805>.
- (35) Radford, A.; Kim, J. W.; Hallacy, C.; Ramesh, A.; Goh, G.; Agarwal, S.; Sastry, G.; Askell, A.; Mishkin, P.; Clark, J.; Krueger, G.; Sutskever, I. Learning Transferable

- Visual Models From Natural Language Supervision. 2021; <https://arxiv.org/abs/2103.00020>.
- (36) van den Oord, A.; Li, Y.; Vinyals, O. Representation Learning with Contrastive Predictive Coding. 2019; <https://arxiv.org/abs/1807.03748>.
- (37) Radford, A.; Wu, J.; Child, R.; Luan, D.; Amodei, D.; Sutskever, I. Language Models are Unsupervised Multitask Learners. 2019.
- (38) Karpathy, A. NanoGPT. <https://github.com/karpathy/nanoGPT>, 2022.
- (39) Jain, A.; Ong, S. P.; Hautier, G.; Chen, W.; Richards, W. D.; Dacek, S.; Cholia, S.; Gunter, D.; Skinner, D.; Ceder, G.; Persson, K. A. Commentary: The Materials Project: A materials genome approach to accelerating materials innovation. *APL Materials* **2013**, *1*, 011002.
- (40) Saal, J. E.; Kirklin, S.; Aykol, M.; Meredig, B.; Wolverton, C. Materials Design and Discovery with High-Throughput Density Functional Theory: The Open Quantum Materials Database (OQMD). *JOM* **2013**, *65*, 1501–1509.
- (41) Scheidgen, M. et al. NOMAD: A distributed web-based platform for managing materials science research data. *Journal of Open Source Software* **2023**, *8*, 5388.

# Supplementary Information

## Hyperparameters and architecture of CatBERTa

Table S1: Overview of CatBERTa’s architecture and training hyperparameters. The CatBERTa encoder retains the same architecture of the publicly available RoBERTa encoder. Identical configurations, except the loss function, are employed in graph-assisted pretraining and the fine-tuning steps.

Hyperparameter	Value
Max positional embeddings	514
Number of attention heads	12
Number of hidden layers	12
Size of each hidden layer	768
Dropout probability in hidden layer	0.1
Batch size	32
Optimizer	AdamW
Scheduler	reduceLR
Initial learning rate	$1 \times 10^{-5}$
Early stopping threshold	5
Warmup steps	0
Loss function	MSE

## Pretraining and Fine-tuning

To evaluate the enhancement from graph-assisted pretraining, we compare the prediction results of CatBERTa with and without this pretraining method, as shown in Table S2. The results are benchmarked using the OC20 and OC20-Dense datasets. The CatBERTa model uses a RoBERTa encoder, which is initially pretrained on a large English corpus using masked language modeling for natural language processing tasks.<sup>19,33</sup> Therefore, when we do not apply graph-assisted pretraining, we directly use RoBERTa, pretrained for natural language processing tasks, as the encoder. In this context, when not applying graph-assisted pretraining, this natural language modeling serves as the pretraining phase. For the energy prediction task, the model is fine-tuned using relaxed energy values as regression labels.

Table S2: CatBERTa pretraining approaches involve data sourced from the OC20 and OC20-Dense datasets, representing the structures in the last frame of DFT relaxations. The term ‘Combined’ refers to the combination of OC20 and OC20-Dense datasets, and ‘GAP’ stands for graph-assisted pretraining.

Enhancement	Pretraining		Fine-tuning	
	Method	Data Source	Method	Data Source
CatBERTa	Masked language modeling	English corpus	Energy prediction	Open Catalyst Dataset
GAP-CatBERTa	Graph-assisted pretraining	Open Catalyst Dataset	Energy prediction	Open Catalyst Dataset

## Alignment in latent space

Our findings demonstrate that graph-assisted pretraining is relatively more effective in clustering systems in the latent space according to their energy levels and adsorbate types, compared to the encoder pretrained with masked language modeling. In Figure S1, the EquiformerV2 embeddings (panels a and d) exhibit distinct clustering for systems with low energy and identical adsorbate types, exemplifying an ideal latent space organization. We presume this clustering precision is associated with the high accuracy of EquiformerV2 in energy predictions. Conversely, the encoder pretrained with masked language modeling results in a more scattered distribution of embeddings (panels b and e), though some degree of clustering exists. Systems with lower energy and nitrogen-containing adsorbates show more pronounced clustering in graph-assisted pretraining, compared to the masked language modeling approach (comparing panels b and c, e and f, respectively). Consequently, graph-assisted pretraining restructures the latent space to reflect the high-performance traits of EquiformerV2, thereby providing a more effective starting point for the subsequent fine-tuning process.

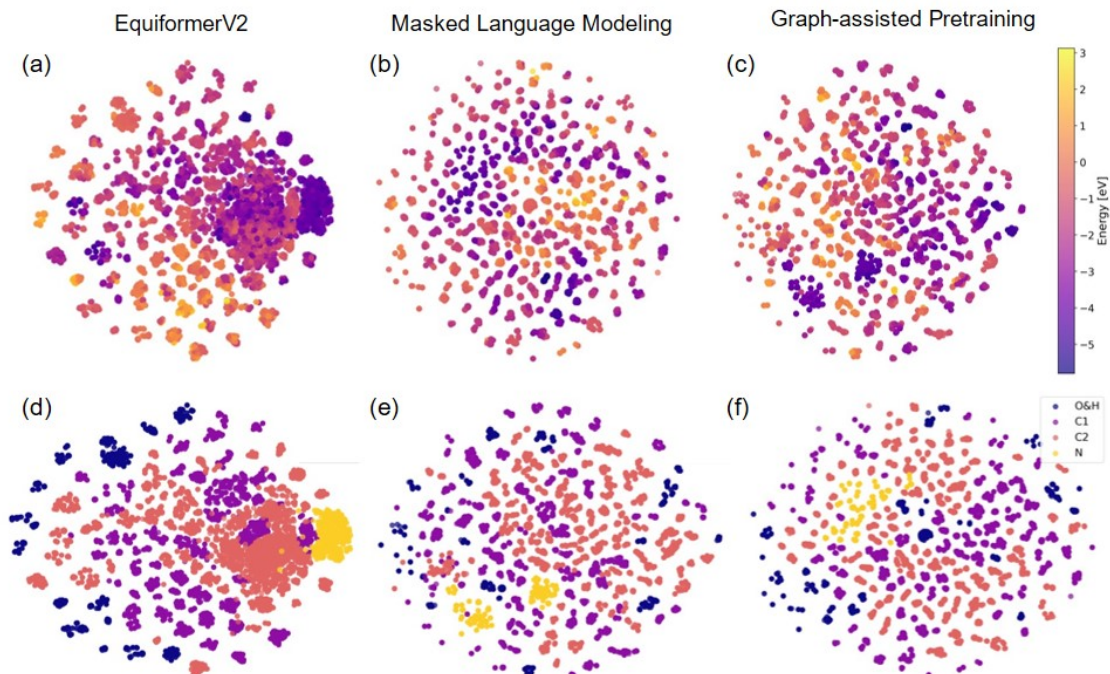


Figure S1: t-SNE visualizations of graph and text embeddings. Graph embeddings are derived from EquiformerV2, while text embeddings are from CatBERTa’s “<s>” token. Upper row panels **a-c** use colors to indicate energy levels, while lower row panels **d-f** color-code by adsorbate type. These adsorbate types are represented as follows: O&H (oxygen/hydrogen), C1 (single carbon-containing adsorbates), C2 (two carbon-containing adsorbates), and N (nitrogen-containing adsorbates)

## Results from diverse ML-relaxed structures



Table S3: CatBERTa prediction results from various ML-relaxed structures as generated by GemNet-OC, SCN, and eSCN.

	MAE [eV] ( $\downarrow$ )			$R^2$ ( $\uparrow$ )		
	GemNet-OC	SCN	eSCN	GemNet-OC	SCN	eSCN
CatBERTa <sub>OC20</sub>	0.696	0.720	0.722	0.597	0.584	0.570
GAP-CatBERTa <sub>OC20</sub>	0.620	0.654	0.656	0.708	0.687	0.679
CatBERTa <sub>combined</sub>	0.373	0.382	0.379	0.868	0.862	0.858
CatBERTa <sub>combined</sub>	0.345	0.351	0.341	0.882	0.880	0.883

## Prediction visualization

The predictions made on GemNet-OC-relaxed structures were selected for example visualization, as shown in Figure S2. The trend follows the results shown in Table 1. The outlier clusters, located at a DFT energy of around -6.5 eV, are adsorption configurations of CHCH adsorbate and  $\text{Ti}_{36}\text{Re}_{18}\text{Os}_{18}$  (0, 0, 1) catalyst. This is likely due to the poor prediction accuracy for the adsorbate CHCH. All entries containing CHCH show an MAE of 0.79 eV for the GAP-CatBERTa<sub>combined</sub> case, which is higher than the MAE for the entire dataset. Although their configurations differ, their energies are very similar, ranging from -6.60 to -6.51 eV, a difference of only 0.12 eV. However, CatBERTa predictions fail to capture this subtle energy difference, showing variations around 0.54 eV. Nevertheless, graph-assisted pretraining can help narrow the prediction range closer to the label energy range. After applying graph-assisted pretraining, the prediction ranges for that outlier cluster are reduced by 37% and 48% for the OC20 training and combined OC20 and OC20-Dense training cases respectively.

The outlier clusters on the right part of the plots are adsorption configurations of the CH adsorbate and  $\text{Ni}_{16}\text{P}_{16}\text{Se}_{48}$  (0, 0, 1) catalyst pair. Systems containing CH show an MAE of 0.40 eV for the GAP-CatBERTa<sub>combined</sub> case, which is not significantly greater than its overall MAE. Thus, this is not attributed to the adsorbates, unlike the previous case. For this cluster, four of the five points share the same configuration strings of [C P Se Se hollow [P Se Se C] [Se Ni Ni C] [Se Ni Ni C]]. It indicates a limitation of the current representation, which

is less sophisticated than the graph representations. Further details about the duplicate configuration strings are provided in the supplementary information.

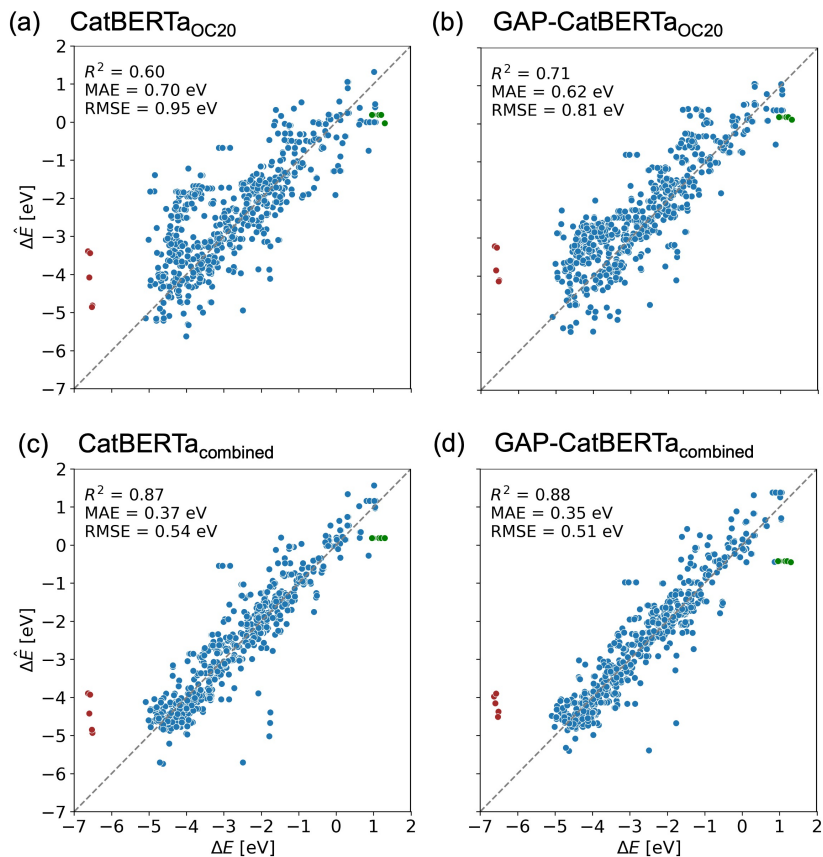


Figure S2: Parity plots comparing DFT-calculated (x-axis) and CatBERTa-predicted (y-axis) energy values for structures relaxed using GemNet-OC. All subfigures are aligned with identical x and y-axes for direct comparison. **a** and **c** show results without graph-assisted pretraining, while **b** and **d** present the results with it.

## Prediction results of duplicate text sets

The textual representation used in this study, which does not fully encode the structure and atomic connectivity, is supposed to be less sophisticated than a graph representation in capturing structural nuances. This limitation is captured in the “Accuracy improvement” section. This limitation is also illustrated in Figure S3(a), where the provided structures exhibit subtle differences that are difficult to discern visually. The graph representation successfully captures these nuances, leading to similar yet distinct configuration energy values for each structure, which range from -2.06 to -2.01 eV. In contrast, our textual representation does not discern these subtle differences, producing identical textual strings for all five structures. Consequently, this leads to identical energy predictions across these structures.

Duplicate texts representing different structures are one of the factors that impact the accuracy of predictions from the CatBERTa model. “Duplicate text sets” refer to those that present the same text for different structures, while “unique text sets” means those with no duplicates. As shown in Figure S3(b), in the CatBERTa<sub>OC20</sub> case, the duplicate text sets exhibit about 40% higher MAE compared to the unique text sets. When graph-assisted pretraining is applied, the accuracy for the duplicate sets improves, along with the unique sets. This suggests that even though textual representations for duplicate sets do not capture subtle structural differences, their overall prediction accuracy can be improved by our pretraining strategy. This observation suggests that refining the textual string to generate distinct texts for similar adsorption configurations could improve CatBERTa’s accuracy.

Additionally, the issue of duplication can be resolved by incorporating additional feature sets that differentiate subtle configurations. In our previous paper, we demonstrated that multiple distinct feature sets could be included in the input data and processed within the same model framework.<sup>19</sup> However, achieving high accuracy with this approach requires identifying feature sets that are highly correlated with the energy of the systems. This identification process is separate from developing a framework that connects graph embeddings and text embeddings. Once these powerful feature sets are identified, we can enhance the

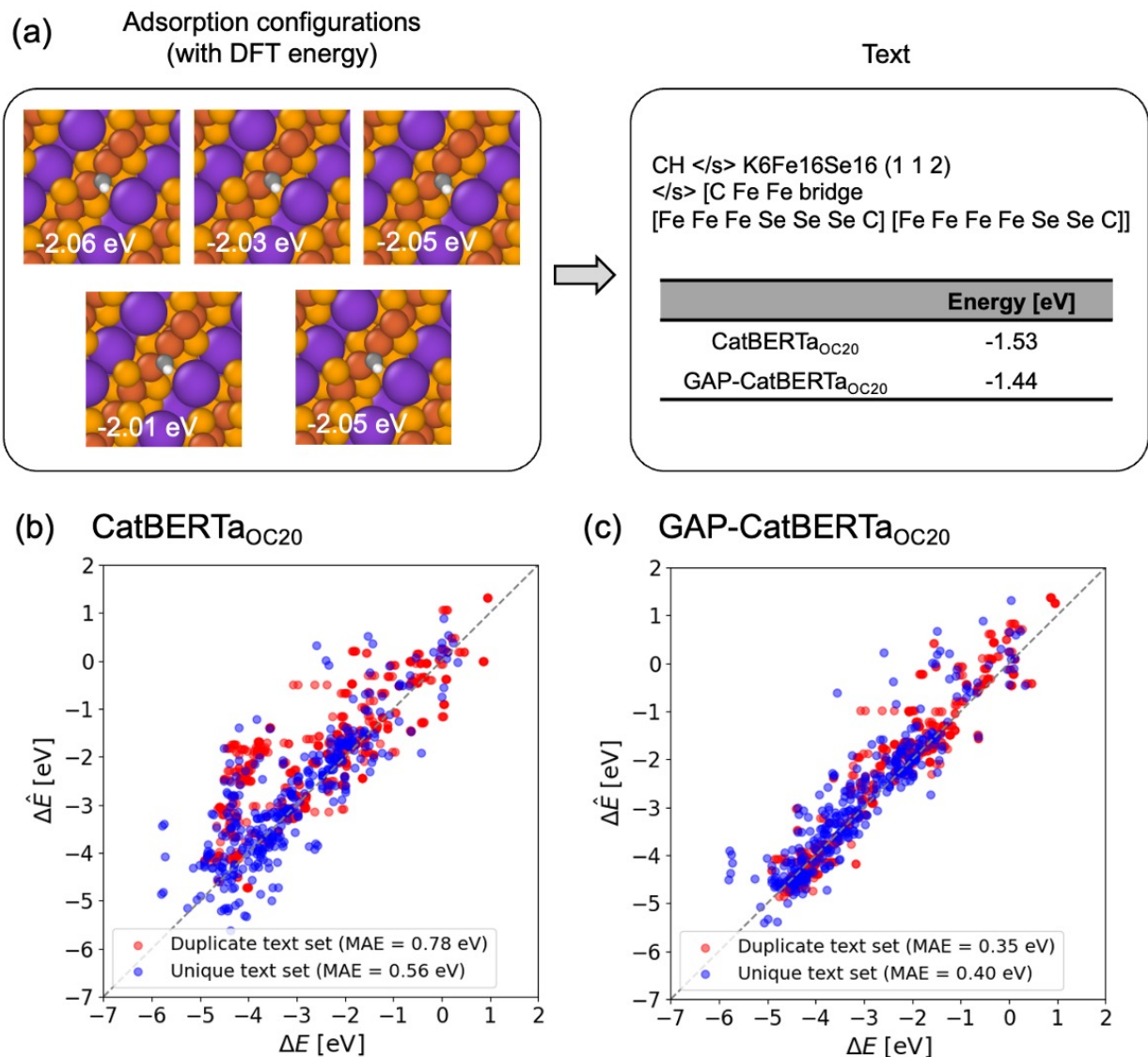


Figure S3: Comparative analysis of prediction performance on duplicate and unique text sets. **a** Instances illustrating the limitation of our textual approach in distinguishing minor structural differences. **b** MAE for each subset, comparing baseline scenarios to cases with enhancements applied.

effectiveness of our text-based approach.

# TOC Graphic

